

## Electrical behavior and Optical Properties of Copper oxide thin Films

*Issam M. Ibrahim\**

*Muhammad O. Salman\**

*Ahmed S.Ahmed \**

Received 3, January, 2011

Accepted 20, May, 2011

### Abstract:

In this work the structural, electrical and optical Properties of CuO semiconductor films had been studied, which prepared at three thickness (100, 200 and 500 nm) by spray pyrolysis method at 573K substrate temperatures on glass substrates from 0.2M  $\text{CuCl}_2 \cdot 2\text{H}_2\text{O}$  dissolved in alcohol. Structural Properties shows that the films have only a polycrystalline CuO phase with preferential orientation in the (111) direction, the dc conductivity shows that all films have two activation energies,  $E_{a1}$  (0.45-0.66 eV) and  $E_{a2}$  (0.055-.0185 eV), CuO films have CBH (Correlated Barrier Hopping) mechanism for ac-conductivity. The energy gap between (1.5-1.85 eV).

**Key words:**TCO materials;Electrical properties;Optical properties;CuO

### Introduction:

CuO is attractive as a selective solar absorber since it has high solar absorbency and a low thermal emittance [1]. Copper forms two well known oxides: cuprite ( $\text{Cu}_2\text{O}$ ) and tenorite (CuO) [2]. The two oxides can coexist with copper, annealing  $\text{Cu}_2\text{O}$  films in air at  $300^\circ\text{C}$  converts it to CuO [3]. While  $\text{Cu}_2\text{O}$  forms a cubic structure with a lattice parameter of 4.27 Å, CuO is unique as it has a square planar coordination of copper by oxygen in the monoclinic structure. The lattice parameters of CuO are  $a = 4.684 \text{ \AA}$ ,  $b = 3.425 \text{ \AA}$ ,  $c = 5.129 \text{ \AA}$  and  $\beta = 99.28^\circ$  [4]. And its suitable optical Properties, Its band gap is reported to be between 1.3 and 1.7 eV with a black color and a partial transparency in the visible range [5]. Due to the existence of copper vacancies in the structure, CuO exhibits native p-type conductivity [6]. Various techniques have been used to synthesize CuO films. Low temperature deposition methods for thin film photovoltaic devices are of

interest to enable the use of lightweight, flexible substrates. Such devices provide a higher power-to-weight ratio and significant cost savings compared to current technologies [7]. The spray pyrolysis method is a well-known thin-film preparation method with excellent features such as the need for no sophisticated equipment, and quality targets or substrates; also, film thickness and stoichiometry are easy to control and the resulting films are well compacted. We have used this coating method to prepare thin films of CuO. Table (1) below shows some of physical properties of Cu, CuO and  $\text{CuCl}_2 \cdot 2\text{H}_2\text{O}$ . [8]. The aim of this work is to illustrate the thickness dependence on optical & electrical properties for CuO and know the mechanism of charge carriers transition.

---

\*University of Baghdad, College of Science, Department of Physics

**Table(1) Mol. weight, physical form, density and qualitative solubility of Cu, CuO and CuCl<sub>2</sub> ·2H<sub>2</sub>O [3]**

Name	Formula	Mol. Weight g/mol	Physical form	Density g/ cm <sup>3</sup>	Qualitative solubility
Copper	Cu	63.546	red metal- cubic	8.96	slightly soluble in dilute acid
Copper(II) oxide	CuO	79.545	black powder or monoclinic crystal	6.31	insoluble in H <sub>2</sub> O, ethanol; soluble dilute acid
Copper(II) chloride dihydrate	CuCl <sub>2</sub> ·2H <sub>2</sub> O	170.482	green-blue orthorhombic crystal; hygroscopic	2.51	Very soluble in ethanol, methanol; soluble in acetone; insoluble in ethyl ether

**Material and Methods:**

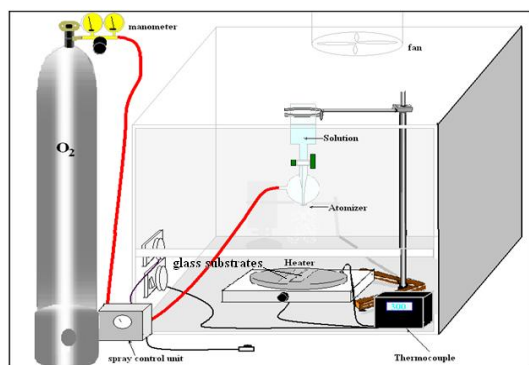
CuO films have been produced by spraying the aqueous solution of 0.2M of CuCl<sub>2</sub> ·2H<sub>2</sub>O onto the microscope glass substrates (1x25x75mm<sup>3</sup>) at substrate temperature of 573K. The substrate temperature was maintained within ±10K. 50 ml alcohol was used for preparing the solutions.

The used CuCl<sub>2</sub> ·2H<sub>2</sub>O weight was calculated using the following equation:

$$\text{Weight (g)} = \text{Molarity (mol/l)} * \text{Volume (l)} * \text{Molecular weight (g/mol)} \dots\dots\dots 1$$

Prior to deposition, the substrates were cleaned with cleaner solution, distilled water and followed by alcohol using ultrasonic bath.

The schematic arrangement of spray pyrolyses set-up is shown in Fig. (1). Spray pyrolysis is basically a chemical process, that is the spraying of the solution onto a substrate held at high temperature, where the solution reacts forming the desired film.

**Fig. (1) Schematic of the spray pyrolysis system.**

The spray rate of the solution was adjusted to be five sprinkling in minute, the sprinkling time about ten second. The normalized distance between the spray nozzle and the substrate is 29cm. Oxygen was used as the carrier gas. The temperature of the substrate was controlled by an Iron-Constantan thermocouple. The thickness of the films (t) was determined using the weighing-method.

$$t = \Delta m / A \rho \dots\dots\dots 2$$

Where  $\Delta m$  = the mass difference of slide after and before the deposition,  $A$  = area =  $2.5 \times 7.5$  cm<sup>2</sup> and  $\rho$  = CuO mass density = 6.31 g/cm<sup>3</sup>.

Crystal structure were investigated by means of a X-ray diffraction XRD Shimadzu 6000 Japan using CuK<sub>α1</sub>,  $\lambda = 1.5405 \text{ \AA}$ ). To study the electrical properties for the films Ohmic contacts for the prepared films are produced by evaporating (Al) electrodes of 300 nm thickness, by means of thermal evaporation methods, using Edward coating unit (model 606) under high vacuum (10<sup>-5</sup> m bar) which was provided by rotary and diffusion pump, then the d.c conductivity ( $\sigma$ ) have been studied using the electrical circuit which is consists of oven type Herease and Keithley (616), while for the a.c conductivity A multi-frequency LRC meters (model HP-R2C 4274A) operated in the 100Hz to 400 KHz frequency range, the specimen was fixed in specimen holder and placed into temperature controlled oven type (Heresies electronic). Three dielectric

parameters were measured directly from above setup total resistance (R), total capacitance (C) and dissipation factor (tanδ) with accuracy of 0.1%. All measurements were performed under certain frequency  $10^2$  - $10^5$  Hz. The temperature range between (303-413K) and constant voltage of (0.08 V) was applied in all frequency range and temperature those are indicated in this work.

The absorbance and the transmittance have been measured for the scanning of electromagnetic spectrum from the range (300-900nm) by the UV visible Philips (Pu 8800 – UV/VIS) spectrophotometer, to calculate from these measurements the energy gap and the other optical constants

**Results and Discussions:**

Fig. (2) Shows XRD for 100,200 and 500 nm thin films deposited on glass from 0.2 M CuCl<sub>2</sub>:2H<sub>2</sub>O. Three peaks can see for (CuO) phase located at  $2\theta=32.49^\circ$  ,  $35.53^\circ$  and  $38.74^\circ$  with hkl (110) , (111) and (111) respectively. The increasing of the thickness approach the structure of the prepared films from the bulk material indicating from increasing of the grain size since the later parameter is inversely proportional with the full width maximum(FWM).

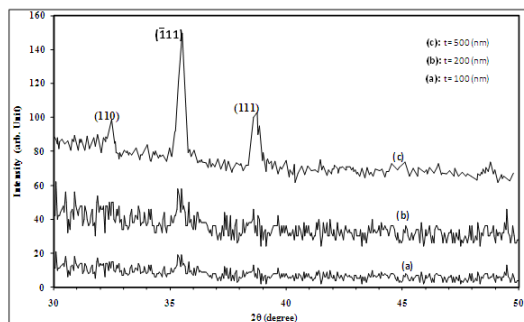


**Fig (2) XRD for 100 ,200and 500 nm CuO deposited on glass**

Table (2) shows the experimental peaks, observe from XRD, and the standard peaks from International

centre for diffraction data (JCPDS) for CuO film and their intensities [9], it shows a perfect identicalness between them.

Table (2) the experimental and the standard peaks from (JCPDS) for CuO film

2θ exp.	d <sub>hkl</sub> Exp.( Å)	Int. %	d <sub>hkl</sub> Std.( Å)	Int. %	hkl
32.49°	2.753	49	2.751	12	(110)
35.53°	2.524	100	2.523	100	(111)
38.74°	2.322	53	2.323	96	(111)
48.76°	1.866	24	1.866	25	(202)

The d.c. conductivity for the films has been studied as a function of temperature at different thicknesses (100, 200 and 500 nm) within the range of (303-508 K) at steep of (10 K) shown in Fig.(3).

D.c conductivity (σ ) of samples obtained using equation (3).

$$\sigma = L/R.td \dots 3$$

where L: distance separated the electrodes, R: Resistance of film, t: film thickness, d: electrodes width.

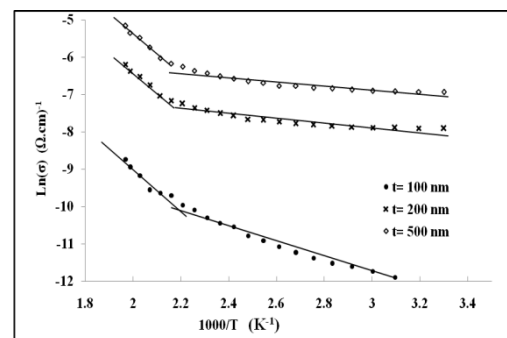


**Fig.(3) The relation between Ln(σ) versus reciprocal of temperature for different film thicknesses (100, 200 and 500nm)**

As seen from Fig.(3) function of ln(σ) versus reciprocal temperature, this figure declared that in all samples there are two stages of conductivity throughout the heating temperature range. The first activation energy (E<sub>a1</sub>) occurs at higher temperature and this

activation energy is due to conduction of the carrier excited into the extended states beyond the mobility edge, while the second activation energy ( $E_{a2}$ ) occurs at low temperature and the conduction mechanism of this stage is due to carriers transport to localized states near the valence and conduction bands. Also we can see the increasing of ( $\sigma$ ) with the increasing of film thickness, this is may be because of increasing the defect states with the increasing the thickness, this is may be attributed to none uniformity in the depth composition.

Table (3) shows the d.c conductivity,  $E_{a1}$  and  $E_{a2}$  for different film thickness. We can notice from this table the activation energy increase with decreasing thickness because the size of the grain decreases with increase the film thickness and that responsible for increase the mean free path of electrons and that lead to increase the conductivity.

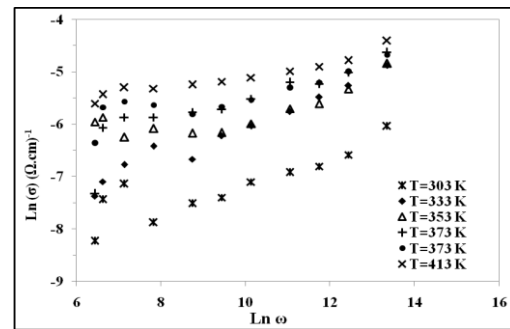
**Table (3) d.c conductivity at R.T,  $E_{a1}$  and  $E_{a2}$  for different film thicknesses**

Thickness (nm)	$\sigma_{RT}$ ( $\Omega.cm$ ) <sup>-1</sup>	Activation energy (eV)		Range (K)
100	$5.48 \cdot 10^{-6}$	$E_{a1}$	0.663	473-508
		$E_{a2}$	0.185	303-473
200	$3.66 \cdot 10^{-4}$	$E_{a1}$	0.470	473-508
		$E_{a2}$	0.059	303-473
500	$9.7 \cdot 10^{-4}$	$E_{a1}$	0.453	473-508
		$E_{a2}$	0.055	303-473

A frequency dependence on a.c conductivity  $\sigma_{a.c}(\omega)$  has been observed in many semiconductors to have the form [10]:

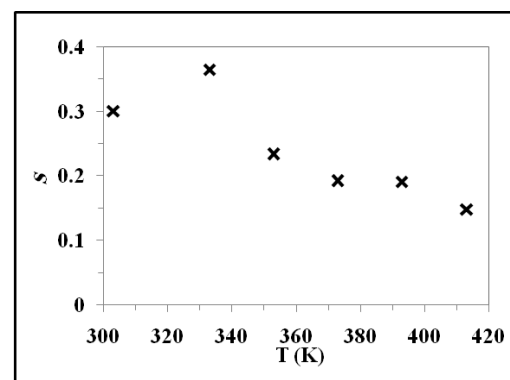
$$\sigma_{a.c}(\omega) = A \omega^s \dots\dots\dots 4$$

Where  $s$  is the exponent factor



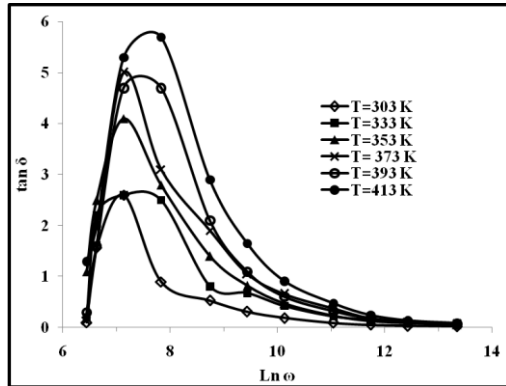
**Fig (4) The relation between  $\text{Ln}(\sigma_{a.c})$  and  $\text{Ln } \omega$  for different temperature.**

Fig. (5) Shows the variation of ac conductivity  $\sigma(\omega)$  as a function of frequency at different temperatures. The conductivity  $\sigma(\omega)$  for all samples increases as frequency becomes greater than 400Hz. In this case the conductivity is proportional to  $\omega^s$ , which means that ac-conductivity dominates at higher frequencies in the range (400Hz-100KHz). For a lower frequencies in the range lower than 400Hz becomes less dependent with frequency, and it is difficult to measure the ac-conductivity component, we found that the value of ( $s$ ) is between (0.14-0.30) when the temperature increases from 303K to 423K. In general, our samples have large values of the exponent ( $s$ ) and it is fit with CBH model given by Long[11] from which ac conduction occurs between two sites over the barrier separating between them as  $D^+D^-$  defect center in the band gap.



**Fig.(5) the variation of the frequency exponent factor with temperature.**

Fig. (6) Illustrates the dielectric loss. In practice, it is convenient to specify the absorption losses in dielectric at a given frequency and temperature by the loss tangent ( $\tan \delta$ ), where  $\delta$  is the angle between the displacement current and its loss components [12]



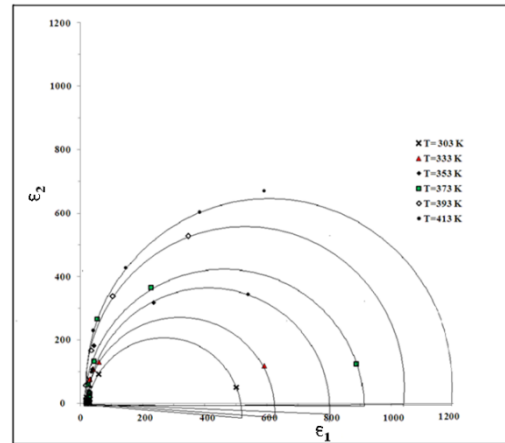
**Fig (6) The variation of dissipation factor with  $\text{Ln} \omega$  for different temperature.**

Fig (7) shows Cole- Cole diagram for CuO films. From this figure we see that the dielectric constant increases with increasing temperatures [see table 4]. To find out the causes of dielectric dispersion such as Debye dispersion; Debye noted that insulating material is usually used over the wide range of frequency and predicated that, when an external alternating field is applied at very high frequencies, the molecular dipoles do not have enough time to change their orientation in keeping with the applied field, since its period necessary to orientate is less than the relaxation time and the dielectric comprises only the contribution from the electronic and ionic polarization. The existent dielectric constant is called optical dielectric constant  $\epsilon_{\infty}$  [13].

Instead at very low frequencies, the period of applied field is very large in comparison with  $\tau$ , the polarization goes to its maximum value, the dielectric constants contain the full contribution from the dipoles

polarization and the power loss is zero [13]. Here dielectric constant is called the static dielectric constant  $\epsilon_s$ .

When an external field  $E$  is applied through dielectric material, the dipoles do not attain its orientation immediately. Also the dipoles polarization requires an amount of time after removal of the external field [14].



**Fig.(7) Cole-Cole diagram at different temperature for.**

**Table (4) exponent factor, polarizability,  $\epsilon_s$  and  $\epsilon_{\infty}$  at different temperatures.**

T (K)	S factor	$\theta$ (deg.)	$\alpha=2\theta/\pi$	P(V/cm)	$\epsilon_s$	$\epsilon_{\infty}$
303	0.301	5	0.055	222.22	310	20
333	0.365	3.9	0.043	173.33	620	24
353	0.235	2.25	0.025	100.00	800	25
373	0.193	0.28	0.003	124.4	910	27
393	0.191	0.24	0.0026	1.066	1040	25
413	0.149	0.21	0.0023	0.933	1200	27

From our data, we conclude that  $\sigma_{ac}(\omega)$  is a function of the temperature of measurements. The values of ac. activation energy  $E_{\omega}$  for CuO films at frequencies

(200,1000,4000,20000,40000 and 100000 Hz) are determined from a plot of  $\ln(\sigma_{ac}(\omega))$  against the reciprocal absolute temperature, as shown in Fig.(8).the temperature dependence of  $\sigma_{ac}$  is logarithmic relation. We can see that there is a weak temperature dependence of  $\sigma_{ac}$  with increasing frequencies in the range (303-413K).[see table 5].

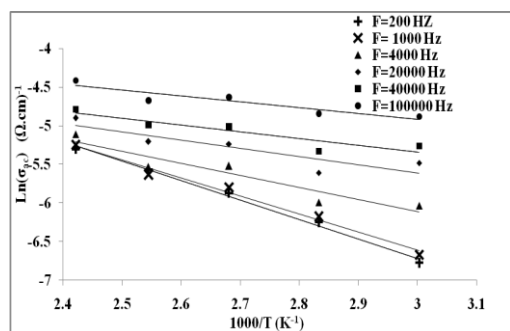


Fig.(8) The relation between  $\text{Ln}(\sigma_{A.C}(\omega))$  versus reciprocal of T

Table (5) A.c activation energy and temperature range for different film thicknesses

F (Hz)	200	1000	4000	20000	40000	100000
$E_a$ (eV)	0.217	0.202	0.135	0.091	0.075	0.064
T Range (K)	333-413	333-413	333-413	333-413	333-413	333-413

Optical study of CuO film is carried out in the wavelength range 200–900 nm at room temperature for the film deposited on glass substrate. Figure (9) shows the room-temperature transmission spectra of three samples at different thicknesses (100, 200 and 500 nm).

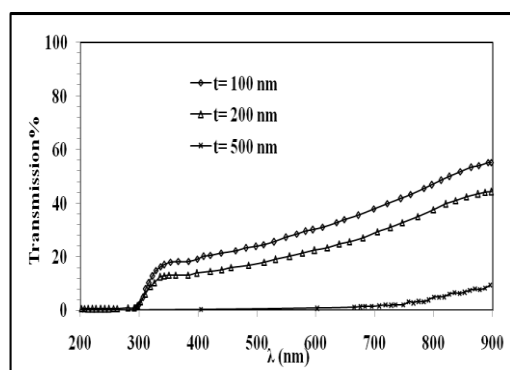


Fig.(9) the transmission variation with the wave length for CuO at different thicknesses

The dependence of the absorption coefficient on the wavelength for different film thicknesses of deposited CuO films on glass is shown in Fig. (10). One can see from this figure that the absorption coefficient of the CuO films is characterized by a strong absorption at the shorter wavelength region which means that there is a

large probability of the allowed direct transition and without sharp edge on the long wavelength side from 350–900 nm.

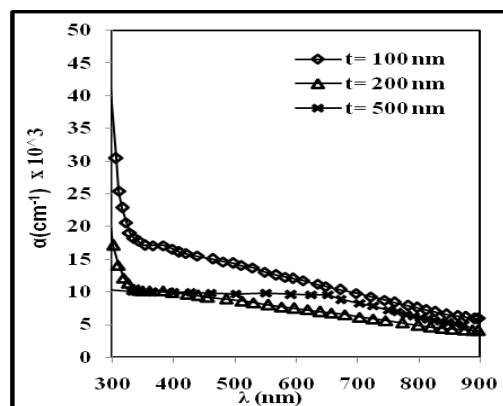


Fig. (10) the variation of absorption coefficient with the wave length for CuO at different thicknesses

The optical energy gap values ( $E_g^{opt}$ ) for CuO films have been determined by using Tauc equation. This is used to find the type of the optical transition by plotting the relations  $(\alpha h\nu)^{1/2}$ ,  $(\alpha h\nu)^{1/3}$ ,  $(\alpha h\nu)^{2/3}$ , and  $(\alpha h\nu)^2$  versus photon energy ( $h\nu$ ). This equation also selects the optimum linear part. It is found that the relation for  $r=1/2$  yields linear dependence, which describes the allowed direct transition.  $E_g^{opt}$  is then determined by the extrapolation of the portion at  $\alpha=0$  as shown in Figure 11), where the values of energy band gap are equal to 1.65, 1.45 and 1.9eV for  $t=100, 200$  and 500nm respectively.

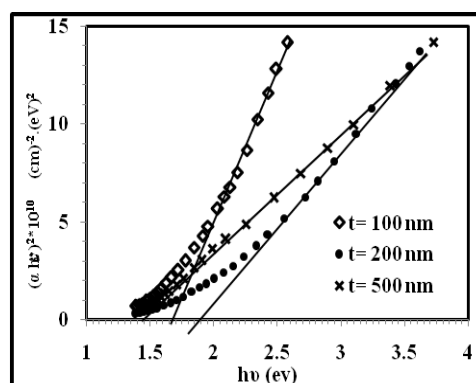


Fig. (11) The variation of  $(\alpha h\nu)^2$  versus photon energy ( $h\nu$ ) for CuO films at different thicknesses.

**Conclusion:**

CuO films were fabricated by chemical spray pyrolysis, with different thickness. The XRD analysis shows that the films were a polycrystalline structure. From dc conductivity investigation we found that the process of conductivity occurs in two stages of conductivity. It has shown that from ac conductivity the exponent ( $s$ ) is temperature dependent [e.g. for  $t=100\text{nm}$  thickness] which found that the value of  $s$  decreases from (0.30 to 0.14), when the temperature increases from 303K to 413K, and the conductivity exponentially dependent on temperature. CBH is most suitable to interpret our results. The optical energy gap indicates not systematic behavior with increasing thicknesses.

**Reference:**

- [1] Yoon K H, Choi W J and Kang D H. 2000. Photo electrochemical properties of copper oxide thin films coated on an n-Si substrate, *Thin Solid Films* 372: 250.
- [2] Richthofen A, Domnic R, Cremer R and Fresenius J. 1997. Preparation of cuprite ( $\text{Cu}_2\text{O}$ ), paramelaconite ( $\text{Cu}_{32}+\text{Cu}_{21}+\text{O}_4$ ) and tenorite ( $\text{CuO}$ ) with magnetron sputtering ion plating, *J. Anal. Chem.* 358: 312-317.
- [3] Pathan H. M. and Lokhande C. D. 2004. Deposition of Metal Chalcogenide Thin Films by Successive Ionic layer Adsorption and Reaction (SILAR) method, *Bull. Mater. Sci.* 27 (2):85-92.
- [4] David R. Lide 2006. CRC Handbook of Chemistry and Physics, ed. Taylor and Francis, Boca Raton, FL.
- [5] Ohya Y, Ito S, Ban T and Takahashi Y. 2000. Preparation of CuO thin films and their electrical conductivity, *Eng. Mater* 181:113-116.
- [6] Jeong Y K and Choi G M. 1996. Nonstoichiometry and electrical conduction of CuO, *Phys. Chem. Solids* 57:81-86.
- [7] Zhang, L., Yu, J. C., Xu A. W., Li Q., Kwong, K. W., Yu S. H. 2004. Peanut-shaped nanoribbon bundle superstructures of malachite and copper oxide, *J. Cryst. Growth* 266: 545-550.
- [8] Cruz M., Herna' L. n, Morales J., Sa' nchez L. 2002. Spray pyrolysis as a method for preparing PbO coatings amenable to use in lead-acid batteries" *Power Sources* 108:35-41.
- [9] JCPDS Data Base, Card No. 05-0661.
- [10] Jonscher A. K. 1976. Alternating current diagnostics of poorly conducting thin films, *Thin Solid Film*, 36: 1-20.
- [11] Davis E.A., Mott N. F. 1979. Electronic processes in non-crystalline materials, Clarendon Press, Oxford : 223.
- [12] Scaife B. K. 1989. Principle of dielectrics, Clarendon press, Oxford. 600.
- [13] Barid M. E. 1989. Electrical properties of dielectric, Clarendon press, Oxford, 455.

## السلوك الكهربائي والخواص البصرية لأغشية اوكسيد النحاس الرقيقة

أحمد صالح أحمد\*

محمد عودة سلمان\*

عصام محمد ابراهيم\*

\*جامعة بغداد, كلية العلوم, قسم الفيزياء

## الخلاصة :

في هذا البحث تم دراسة الخصائص التركيبية والكهربائية والبصرية لأغشية CuO المحضرة بثلاث اسماك (t=100,200 and 500 nm) بطريقة الرش الكيميائي عند درجة حرارة ارضية 573K على ارضيات من الزجاج من محلول 0.2 مولاري من  $CuCl_2 \cdot 2H_2O$  مذاب في 50 مليلتر من الكحول. أظهرت الفحوصات التركيبية ان الأغشية المحضرة لها تركيب متعدد التبلور وبدورانية باتجاه (111). اما قياسات التوصيلية المستمرة فتظهر بان الأغشية لها منطقتين لطاقة  $(E_{a1}=0.45-(0.66eV)$  ,  $(E_{a2}=0.05-0.85eV)$  . أما نتائج التوصيلية المتناوبة فأظهرت ان الأغشية المحضرة تخضع لنموذج تنطط الحاجز المتلازم (CBH) , أما فجوة الطاقة فكانت تتراوح بين  $(E_g=1.5-1.85 eV)$